

# Sensitivity of coccolithophores to carbonate chemistry and ocean acidification

L. Beaufort<sup>1</sup>, I. Probert<sup>2</sup>, T. de Garidel-Thoron<sup>1</sup>, E. M. Bendif<sup>2</sup>, D. Ruiz-Pino<sup>3</sup>, N. Metz<sup>1</sup>, C. Goyet<sup>4</sup>, N. Buchet<sup>1</sup>, P. Coupel<sup>3</sup>, M. Grelaud<sup>1†</sup>, B. Rost<sup>5</sup>, R. E. M. Rickaby<sup>6</sup> & C. de Vargas<sup>2</sup>

About one-third of the carbon dioxide (CO<sub>2</sub>) released into the atmosphere as a result of human activity has been absorbed by the oceans<sup>1</sup>, where it partitions into the constituent ions of carbonic acid. This leads to ocean acidification, one of the major threats to marine ecosystems<sup>2</sup> and particularly to calcifying organisms such as corals<sup>3,4</sup>, foraminifera<sup>5–7</sup> and coccolithophores<sup>8</sup>. Coccolithophores are abundant phytoplankton that are responsible for a large part of modern oceanic carbonate production. Culture experiments investigating the physiological response of coccolithophore calcification to increased CO<sub>2</sub> have yielded contradictory results between and even within species<sup>8–11</sup>. Here we quantified the calcite mass of dominant coccolithophores in the present ocean and over the past forty thousand years, and found a marked pattern of decreasing calcification with increasing partial pressure of CO<sub>2</sub> and concomitant decreasing concentrations of CO<sub>3</sub><sup>2–</sup>. Our analyses revealed that differentially calcified species and morphotypes are distributed in the ocean according to carbonate chemistry. A substantial impact on the marine carbon cycle might be expected upon extrapolation of this correlation to predicted ocean acidification in the future. However, our discovery of a heavily calcified *Emiliania huxleyi* morphotype in modern waters with low pH highlights the complexity of assemblage-level responses to environmental forcing factors.

To assess the influence of the environment on coccolithophore calcification, we investigated 180 surface-water and 555 sediment-core samples encompassing a wide spectrum of present and past oceanic conditions (Fig. 1). The family Noëlaerhabdaceae (including the extant genera *Emiliania*, *Gephyrocapsa* and *Reticulofenestra*) has dominated coccolithophore communities numerically for more than 20 million years. Although they are closely related genetically<sup>12</sup>, noëlaerhabdaceans vary both between and within species in the morphology of the calcite scales (coccoliths) that form their composite skeletons (coccospheres)<sup>13</sup>. An optical method for automatic analysis of the size and mass of individual noëlaerhabdacean coccospheres and detached coccoliths was applied, with an average of 700 coccoliths measured per sample. The mass of isolated coccoliths was strongly correlated with the mass of coccospheres in modern samples ( $R^2 = 0.88$ ), demonstrating the validity of coccolith mass as a proxy for the calcification state of noëlaerhabdaceans.

Temperature, salinity, alkalinity and dissolved inorganic carbon were recorded directly from modern water samples, allowing the derivation of all carbonate-chemistry parameters<sup>14</sup>. To reconstruct the carbonate chemistry of surface waters in the past, published palaeo-proxy records for sea surface temperature and salinity from each core site were combined with records of CO<sub>2</sub> partial pressure ( $p_{\text{CO}_2}$ ) from Antarctic ice. Uncertainties due to the propagation of errors from temperature and salinity estimates, and from our assumption of stability over the past 40,000 years (kyr) in relationships linking

alkalinity and salinity, the ratio of stable oxygen isotopes ( $\delta^{18}\text{O}$ ) in water and salinity, and  $p_{\text{CO}_2}$  in water and in the atmosphere, had only a limited effect on the general trend (Supplementary Information). The resulting glacial–interglacial ranges of carbonate-chemistry parameters are similar to those published elsewhere<sup>5,15</sup>.

Temperature, salinity, light and nutrients have all been reported to affect coccolithophore calcification or coccolith size<sup>13,16–20</sup>. Analysis of our large data set reveals that temperature and salinity are not strongly correlated with coccolith mass. The contrasting correlations between coccolith mass and temperature in modern samples ( $R = 0.59$ ) and in sediment samples ( $R$  between  $-0.12$  and  $-0.71$ ) reflect the differing relationship between temperature and carbonate concentration ( $[\text{CO}_3^{2-}]$ ) in modern and past oceans (Table 1). No significant correlations were found between coccolith mass and productivity-related parameters (chlorophyll or cell abundance), where these were available.

Coccolith mass was related to carbonate chemistry. Significant overall correlations of coccolith mass with pH and  $p_{\text{CO}_2}$  were recorded, but with notable regional variations (Fig. 1c), indicating that these parameters are not solely responsible for the observed trend. The only correlations that were highly significant in all subsets of the data were those linking coccolith mass to  $[\text{CO}_3^{2-}]$ ,  $[\text{HCO}_3^-]$  and calcite saturation state ( $\Omega_{\text{Ca}}$ ) ( $R^2 > 0.74$ , Fig. 1b and Table 1). The influence of carbonate chemistry was particularly notable in sediment records: during the Last Glacial Maximum,  $p_{\text{CO}_2}$  was low ( $[\text{CO}_3^{2-}]$  was high) and coccolith mass was high (Fig. 2). During deglaciation and the Holocene epoch, coccolith mass decreased with increasing  $p_{\text{CO}_2}$  at all latitudes in different ocean basins. This trend cannot have resulted from post-depositional corrosion because glacial–interglacial dissolution conditions evolved in opposite directions in the Atlantic and Pacific oceans<sup>21</sup>. A significant correlation was also found between  $[\text{CO}_3^{2-}]$  and amount of calcite per unit cell volume ( $R^2 = 0.76$ ), indicating that the degree of calcification was not dependent on cell size. There was a negative correlation between calcite mass and  $[\text{HCO}_3^-]$ , despite this anion being the primary carbon source for intracellular calcification in *E. huxleyi*<sup>16,22,23</sup>.  $[\text{HCO}_3^-]$  varied by about 20% in our data set, but it is the most abundant carbon species in sea water and is therefore unlikely to limit biomineralization. In contrast,  $[\text{CO}_3^{2-}]$  varied by 77%. Several physico-chemical parameters could synergistically affect calcification, but multiple regression did not markedly increase the significance of the correlation of coccolith mass with  $[\text{CO}_3^{2-}]$ . Although various parameters clearly exert a localized influence on coccolith mass, our data point to  $[\text{CO}_3^{2-}]$  and  $\Omega_{\text{Ca}}$  being key parameters in the global assemblage-scale response of noëlaerhabdacean calcification to ocean acidification.

We next explored what drives the trend linking calcification and carbonate chemistry. The results of monoclonal culture experiments, showing a decrease in noëlaerhabdacean calcification (degree and rate) with ocean acidification (for example, refs 8 and 11) have focused

<sup>1</sup>CEREGE, CNRS/Université Aix-Marseille, Avenue L. Philibert BP80, 13545 Aix-en-Provence, Cedex 4, France. <sup>2</sup>Station Biologique de Roscoff, CNRS/Université P. & M. Curie, Place G. Teissier, 29680 Roscoff, France. <sup>3</sup>LOCEAN-IPSL, CNRS/Université P. & M. Curie, BP 100, 4 Place Jussieu, 75252 Paris, Cedex 5, France. <sup>4</sup>Université de Perpignan, 52 Avenue P. Alduy, 66860 Perpignan, Cedex 9, France. <sup>5</sup>Alfred Wegener Institute, Am Handelshafen 12, 27570 Bremerhaven, Germany. <sup>6</sup>Oxford University, Department of Earth Sciences, Parks Road, Oxford OX1 3OR, UK. <sup>†</sup>Present address: ICTA, Universitat Autònoma de Barcelona, 08193 Bellaterra, Spain.

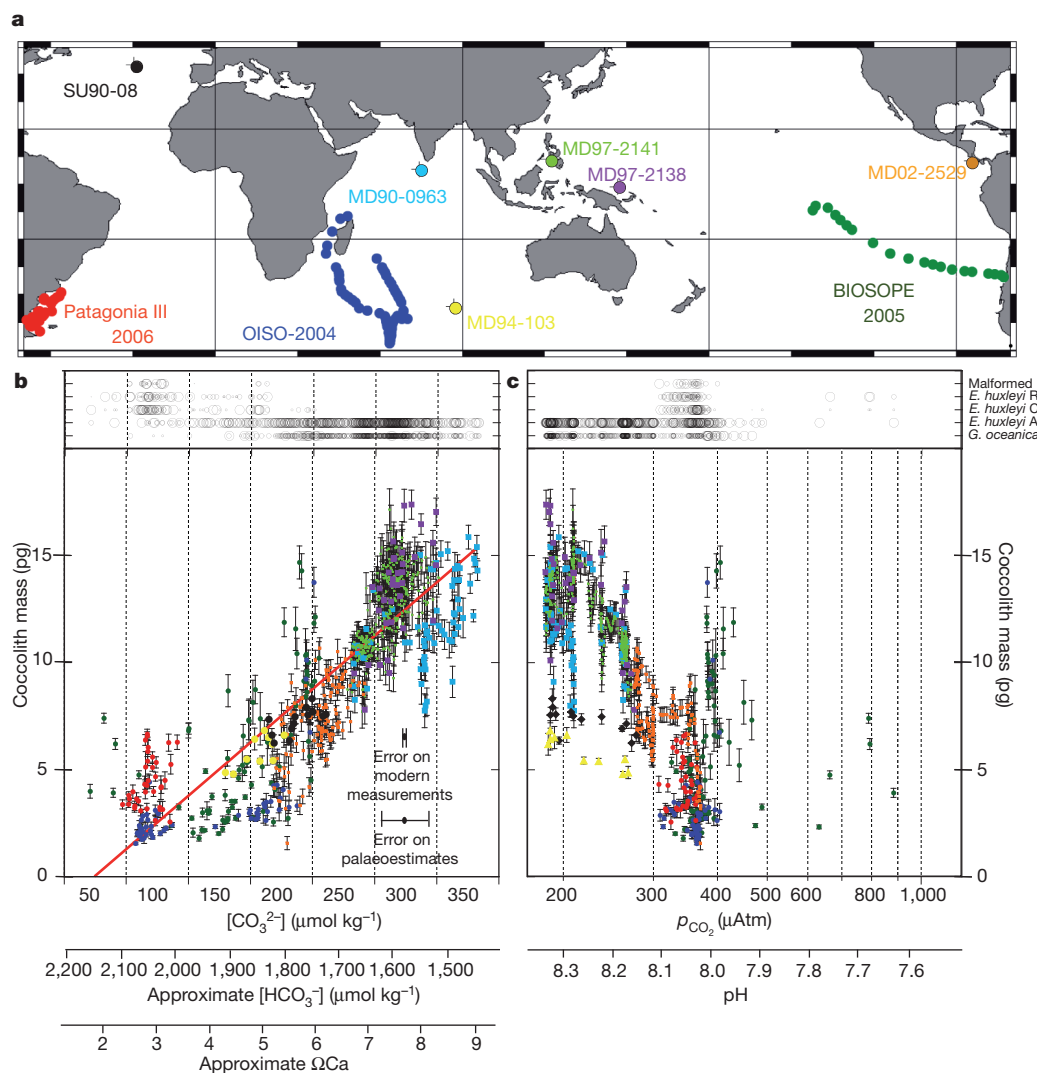


**Figure 1 | Relationships between coccolith mass and carbonate chemistry.** **a**, Map of sample locations. **b**, Relationship between  $[\text{CO}_3^{2-}]$  and coccolith mass (colours correspond to those on the map in **a**). Vertical bars are standard error on the mass distribution. For comparison, the corresponding scales for  $\Omega\text{Ca}$  and  $[\text{HCO}_3^-]$  are shown. Error bars for  $[\text{CO}_3^{2-}]$  are estimated from modern and past data. **c**, Relationship between coccolith mass and  $p_{\text{CO}_2}$  in water. The corresponding pH scale is given. Upper panels in **b** and **c** show qualitative distribution of noëlarhabdacean taxa: large circles for dominant taxa (>50%), medium circles for abundant taxa (30–50%) and small circles for less abundant taxa (10–30%).

attention on the existence of a direct, environmentally mediated physiological constraint on calcification. Coccoliths are secreted intracellularly in coccolith-producing vesicles in which pH and  $\Omega\text{Ca}$  are maintained at levels that stimulate calcite precipitation. Several explanations have been proposed to explain decreased calcification rates with ocean acidification<sup>24</sup>, for example, that the necessary outward transport of protons may become more costly in low-pH and/or low- $[\text{CO}_3^{2-}]$  waters<sup>25</sup>. The environmental relevance of such a physiological mechanism cannot be resolved directly from our data, but in culture experiments, the maximum decrease in mass of a clone over carbonate-chemistry ranges comparable to those of our data set is about 20%: only a fraction of the total response in our data set. In addition, some cultured strains of noëlarhabdaceans and other coccolithophores are capable of maintaining calcification (degree and/or

rate) over certain carbonate-chemistry ranges, a phenomenon that could contribute to localized within-sample deviations from the broad trend linking coccolith mass to carbonate chemistry.

A general physiological mechanism is evidently insufficient to explain the overall decline in coccolith mass in our data set. The three noëlarhabdacean genera include several species, each with a number of morphological variants (morphotypes)<sup>26</sup>. In our global sample set, the lightest *E. huxleyi* (morphotype C) was present in waters with  $[\text{CO}_3^{2-}] < 200 \mu\text{mol kg}^{-1}$ , whereas the heavy *Gephyrocapsa oceanica* (which includes several morphotypes<sup>13</sup>) only occurred in waters above this concentration (Fig. 1b). *Emiliania huxleyi* with intermediate mass (morphotypes A and B) occupied wider and intermediate  $[\text{CO}_3^{2-}]$  ranges. Significant coccolith malformation occurred at low  $[\text{CO}_3^{2-}]$  in *E. huxleyi* morphotype C from the Patagonian shelf and Antarctic

**Table 1 | Correlation between coccolith mass and physicochemistry**

Sample set	Temperature	Salinity	Alkalinity	DIC	pH	$p_{\text{CO}_2}$	$\text{HCO}_3^-$	$\text{CO}_3^{2-}$	$\Omega\text{Ca}$	<i>n</i>
All data	<b>0.68</b>	<b>0.27</b>	<b>0.13</b>	<b>-0.82</b>	<b>0.75</b>	<b>-0.69</b>	<b>-0.87</b>	<b>0.86</b>	<b>0.86</b>	712
BIOSOPE	<b>0.77</b>	<b>0.58</b>	<b>0.63</b>	-0.02	<b>-0.52</b>	<b>0.53</b>	<b>-0.57</b>	<b>0.71</b>	<b>0.72</b>	84
PATAGONIA	0.31	0.18	0.14	0.03	0.04	0.01	-0.11	0.26	0.26	39
OISO-11	<b>0.65</b>	0.32	0.19	<b>-0.68</b>	-0.31	0.29	<b>-0.65</b>	<b>0.60</b>	<b>0.61</b>	57
MD90-0963	-0.12	<b>0.62</b>	<b>0.63</b>	<b>0.60</b>	0.37	-0.33	-0.07	<b>0.53</b>	<b>0.52</b>	68
MD97-2141	<b>-0.71</b>	-0.15	-0.12	<b>-0.68</b>	<b>0.79</b>	<b>-0.80</b>	<b>-0.75</b>	<b>0.67</b>	<b>0.67</b>	305
MD97-2138	-0.34	0.11	0.13	-0.41	<b>0.59</b>	<b>-0.60</b>	<b>-0.60</b>	<b>0.65</b>	<b>0.65</b>	35
MD02-2529	<b>-0.48</b>	<b>0.45</b>	<b>0.48</b>	0.23	<b>0.62</b>	<b>-0.62</b>	-0.23	<b>0.61</b>	<b>0.61</b>	124
MD94-103	-0.80	0.00	0.12	-0.50	<b>0.88</b>	<b>-0.87</b>	-0.75	0.64	0.67	9
SU90-08	-0.40	0.60	0.59	0.02	0.64	-0.65	-0.41	<b>0.68</b>	<b>0.68</b>	18

Significant correlation coefficient values are set in bold. *n*, number of samples in a given set.

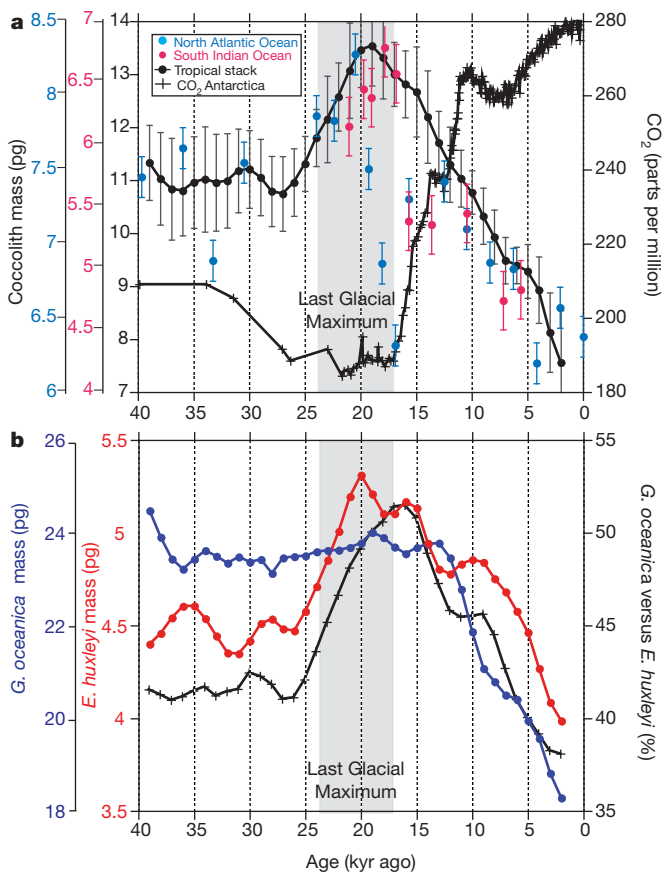


**Figure 2 | Variation of coccolith mass, species composition and CO<sub>2</sub> concentration over the last 40 kyr.** **a**, Coccolith mass (filled circles) in the low-latitude (tropical) stack is shown in black (average of the four records, error bars are standard error between records). Coccolith mass at sample site MD94-103 (South Indian Ocean) is shown in red and at site SU90-08 (North Atlantic Ocean), in blue (error bars show standard error in each sample). The CO<sub>2</sub> concentration in ice cores at EPICA<sup>29</sup> (0–22 kyr) and Vostok<sup>30</sup> (22–40 kyr) is represented by crosses. **b**, Measurements of coccolith mass in the low-latitude stack, showing *G. oceanica* in blue, *E. huxleyi* in red and the relative abundance of the two taxa in black. Grey shading marks the period of the Last Glacial Maximum.

ocean. Changes in the relative abundance of taxa were therefore predominantly responsible for the decrease in coccolith mass with ocean acidification that was seen in modern samples. Both *Gephyrocapsa* and *Emiliania* showed a decrease in coccolith mass of about 25% from the Last Glacial Maximum to the near-present, paralleling an increase in CO<sub>2</sub> of about 100 parts per million by volume (Fig. 2). In addition to a physiological response of individual morphotypes, this could have resulted from changes in the abundance of different morphotypes within the genera. Superimposed on this intra-generic response, a decrease in relative abundance of *Gephyrocapsa* versus *Emiliania* was the main factor underlying the overall mass variation over the last 40 kyr (Fig. 2b). Although the function of coccoliths is unknown, our data indicate that variability in calcite mass (or the associated energy expenditure) is subject to ecological selective pressure.

We observed a key exception to the global correlation between noëlaerhabdacean calcification and [CO<sub>3</sub><sup>2-</sup>]. In Patagonian-shelf and Chilean upwelling waters with low [CO<sub>3</sub><sup>2-</sup>], in which the overall trend would predict low coccolith mass, we detected an unexpectedly highly calcified *E. huxleyi* morphotype (Fig. 1b), reminiscent of morphotype R<sup>26</sup>. The relative abundance of this morphotype increased with decreasing pH along the Pacific transect towards Chile (Fig. 3). Many environmental gradients exist along this transect, leading to the correlation of several factors with calcite mass, with mutual interactions (see for example ref. 18) that potentially mask the typical

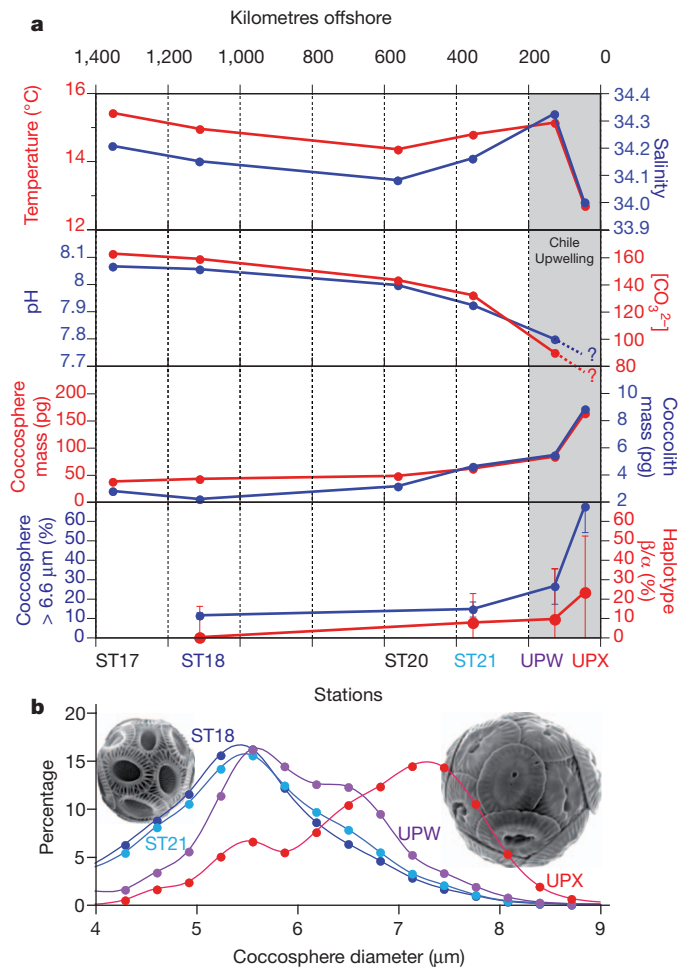


**Figure 3 | Physico-chemical and coccolithophore variability along an east-west acidity gradient in the south-east Pacific.** Data are from the biogeochemistry and optics South Pacific experiment (BIOSOPE) (station averages of values are given in Supplementary Table 2). **a**, Plots of temperature and salinity, [CO<sub>3</sub><sup>2-</sup>] and pH (water chemistry was not measured at station UPX), mass of coccospheres and coccoliths, and percentages of large coccospheres (>6.6 μm) and of haplotype β versus α. Error bars are confidence intervals at 95%. **b**, Distribution of coccosphere diameters at different stations. ST18 ( $n = 1,334$ ), ST21 ( $n = 578$ ), UPW ( $n = 210$ ), UPX ( $n = 203$ ). Typical coccospheres of *E. huxleyi* type A (left, from ST18) and *E. huxleyi* type R (right, from UPX) are shown.

response of mass to carbonate chemistry. Alternatively, because coccolith morphotype is thought to be subject to genetic regulation<sup>11</sup>, this highly calcified *E. huxleyi* morphotype may be a genetic entity with an adaptation enabling it to calcify heavily in the relatively acidic upwelling waters. In this context, we note that the only culture study that reported an increase in *E. huxleyi* calcification with ocean acidification was conducted with a morphotype-R strain<sup>9</sup>.

To probe the genetic diversity of *E. huxleyi*, we generated clone libraries from samples collected along the acidity gradient that characterizes offshore Chilean water masses. We detected a shift in the relative abundance of two distinct mitochondrial haplotypes of *E. huxleyi* that coincided with the shift in relative abundance of morphotypes along the transect (Fig. 3). Each haplotype has wide oceanic distribution (Supplementary Information), indicating that the observed distribution is not the result of regional endemism. The relationship between mitochondrial haplotypes and morphotype is not, however, straightforward<sup>27</sup>, and establishing a strict link between morphotypic and genotypic diversities requires further environmental morphogenetic studies and/or culture-based physio-genomic comparisons. The presence of highly calcified *E. huxleyi* in these samples does not mask

the main pattern of decreasing calcification at low  $[\text{CO}_3^{2-}]$ , but highlights the fact that coccolithophores can calcify heavily at low pH (7.62) and low  $[\text{CO}_3^{2-}]$  ( $71 \mu\text{mol kg}^{-1}$ ).

Coccolithophore calcification may be influenced by several factors, but our environmental data show a spatio-temporally consistent decline of coccolith mass with decreasing  $[\text{CO}_3^{2-}]$ . Integrating this coccolithophore response with the predicted decrease in calcification of planktonic foraminifera<sup>6,7</sup> and neritic corals<sup>3,4</sup> under conditions of increased  $\text{CO}_2$  means that entire marine calcifying communities seem likely to be affected in the future. However, the presence of highly calcified *E. huxleyi* in  $\text{CO}_2$ -rich modern waters demonstrates that prediction of future responses is unlikely to be straightforward. Such complexity could account for the lack of an obvious overall direction in the response of coccolithophore calcification over a potentially analogous ocean acidification event about 55 million years ago at the Palaeocene–Eocene Thermal Maximum<sup>28</sup>. Attention should now focus not only on the physiological response of individual strains to changing carbonate chemistry, but also on characterizing responses in complex assemblages.

## METHODS SUMMARY

Image analyses were performed on 40 frames ( $240 \times 180 \mu\text{m}$  with a pixel area of  $0.0225 \mu\text{m}^2$ ) per microscope slide, selected using an automated microscope (Leica DMRBE). Coccoliths and coccospheres were detected, classified and morphometrically analysed by the SYRACO software, which performs pattern recognition using artificial neural networks. Mass was estimated by measuring brightness in cross-polarized light (birefringence), with brightness being converted into mass after calibration with calcite microspheres of known mass.

Water sampling and measurements of temperature and salinity on three oceanographic cruises were conducted onboard. Total dissolved inorganic carbon (DIC) and total alkalinity (TA) were determined by the potentiometric acid titration method. To infer past changes in surface ocean-carbonate-system values, salinity and TA values in the past were estimated from geochemical proxies of past surface hydrography, using published estimates of past sea surface temperature and measured  $\delta^{18}\text{O}$ . Surface  $p_{\text{CO}_2}$  was estimated using atmospheric  $p_{\text{CO}_2}$  values measured in Antarctic ice cores at Vostok and EPICA, which are considered to represent global values throughout the temporal range of our records. Other carbonate-chemistry parameters were calculated using the CO2sys software with temperature, salinity, TA and DIC as inputs.

For genetic analyses, 10-litre seawater samples were filtered onto nucleopore membranes (Millipore). Total DNA was extracted using the DNeasy Plant mini kit (Qiagen) and *cox3* sequences were amplified using the Phusion High-Fidelity PCR mix (New England Biolabs). PCR primers are given in the Supplementary Information. For construction of environmental clone libraries, amplified sequences were inserted into the TOPO-TA PCR 4 vector (Invitrogen) before transformation into competent cells. PCR products were sequenced directly using the ABI PRISM BigDye Terminator Cycle Sequencing Kit on an ABI PRISM 3100 xl auto sequencer (Applied Biosystems). Maximum likelihood analysis was performed in TREEFINDER using manually aligned 812-base-pair *cox3* sequences under the corrected Akaike information criterion model.

Received 20 July 2010; accepted 15 June 2011.

- Sabine, C. L. *et al.* The oceanic sink for anthropogenic  $\text{CO}_2$ . *Science* **305**, 367–371 (2004).
- Fabry, V. J., Seibel, B. A., Feely, R. A. & Orr, J. C. Impacts of ocean acidification on marine fauna and ecosystem processes. *ICES J. Mar. Sci.* **65**, 414–432 (2008).
- Gattuso, J.-P., Frankignoulle, M., Bourge, I., Romaine, S. & Buddemeier, R. W. Effect of calcium carbonate saturation of seawater on coral calcification. *Global Planet. Change* **18**, 37–46 (1998).
- Kleypas, J. A. *et al.* Geochemical consequences of increased atmospheric carbon dioxide on coral reefs. *Science* **284**, 118–120 (1999).
- Barker, S. & Elderfield, H. Foraminiferal calcification response to glacial–interglacial changes in atmospheric  $\text{CO}_2$ . *Science* **297**, 833–836 (2002).
- Moy, A. D., Howard, W. R., Bray, S. G. & Trull, T. W. Reduced calcification in modern Southern Ocean planktonic foraminifera. *Nature Geosci.* **2**, 276–280 (2009).
- de Moel, H. *et al.* Planktic foraminiferal shell thinning in the Arabian Sea due to anthropogenic ocean acidification? *Biogeosciences* **6**, 1917–1925 (2009).
- Riebesell, U. *et al.* Reduced calcification of marine plankton in response to increased atmospheric  $\text{CO}_2$ . *Nature* **407**, 364–367 (2000).
- Iglesias-Rodriguez, M. D. *et al.* Phytoplankton calcification in a high- $\text{CO}_2$  world. *Science* **320**, 336–340 (2008).
- Langer, G. M. *et al.* Species-specific responses of calcifying algae to changing seawater carbonate chemistry. *Geochem. Geophys. Geosyst.* **7**, Q09006 (2006).

- Langer, G., Nehrke, G., Probert, I., Ly, J. & Ziveri, P. Strain-specific responses of *Emiliania huxleyi* to changing seawater carbonate chemistry. *Biogeosci. Discuss.* **6**, 4361–4383 (2009).
- de Vargas, C., Aubry, M. P., Probert, I. & Young, J. in *Evolution of Aquatic Photoautotrophs* (eds Falkowski, P. G. & Knoll, A. H.) 251–285 (Academic, 2007).
- Bollmann, J., Henderiks, J. & Brabec, B. Global calibration of *Gephyrocapsa* coccolith abundance in Holocene sediments for paleotemperature assessment. *Paleoceanogr.* **17**, doi:10.1029/2001PA000742 (2002).
- Lewis, E. & Wallace, D. W. R. Program developed for  $\text{CO}_2$  system calculations. *Carbon Dioxide Information and Analysis Center Report, ORNL/CDIAC-105* (1998).
- Hönisch, B. & Hemming, N. G. Surface ocean pH response to variations in  $p_{\text{CO}_2}$  through two full glacial cycles. *Earth Planet. Sci. Lett.* **236**, 305–314 (2005).
- Paasche, E. A review of the coccolithophorid *Emiliania huxleyi* (Prymnesiophyceae), with particular reference to growth, coccolith formation, and calcification–photosynthesis interactions. *Phycologia* **40**, 503–529 (2001).
- Zondervan, I. The effects of light, macronutrients, trace metals and  $\text{CO}_2$  on the production of calcium carbonate and organic carbon in coccolithophores—a review. *Deep Sea Res. II* **54**, 521–537 (2007).
- Feng, Y. *et al.* Interactive effects of increased  $p_{\text{CO}_2}$ , temperature and irradiance on the marine coccolithophore *Emiliania huxleyi* (Prymnesiophyceae). *Eur. J. Phycol.* **43**, 87–98 (2008).
- Bollmann, J. & Herrle, J. O. Morphological variation of *Emiliania huxleyi* and sea surface salinity. *Earth Planet. Sci. Lett.* **255**, 273–288 (2007).
- Colmenero-Hidalgo, E., Flores, J. A. & Sierro, F. J. Biometry of *Emiliania huxleyi* and its biostratigraphic significance in the Eastern North Atlantic Ocean and Western Mediterranean Sea in the last 20 000 years. *Mar. Micropaleontol.* **46**, 247–263 (2002).
- Anderson, D. M. & Archer, D. Glacial interglacial stability of ocean pH inferred from foraminifer dissolution rates. *Nature* **416**, 70–73 (2002).
- Buitenhuis, E. T., de Baar, H. J. W. & Veldhuis, M. J. W. Photosynthesis and calcification by *Emiliania huxleyi* (Prymnesiophyceae) as a function of inorganic carbon species. *J. Phycol.* **35**, 949–959 (1999).
- Berry, L., Taylor, A. R., Lucken, U., Ryan, K. P. & Brownlee, C. Calcification and inorganic carbon acquisition in coccolithophores. *Funct. Plant Biol.* **29**, 289–299 (2002).
- Mackinder, L., Wheeler, G., Schroeder, D., Riebesell, U. & Brownlee, C. Molecular mechanisms underlying calcification in coccolithophores. *Geomicrobiol. J.* **27**, 585–595 (2010).
- Zondervan, I., Rost, B. & Riebesell, U. Effect of  $\text{CO}_2$  concentration on the PIC/POC ratio in the coccolithophore *Emiliania huxleyi* grown under light-limiting conditions and different daylengths. *J. Exp. Mar. Biol. Ecol.* **272**, 55–70 (2002).
- Young, J. *et al.* A guide to extant coccolithophore taxonomy. *J. Nannoplankton Res.* **1** (Special Issue), 1–132 (2003).
- Hagino, K. *et al.* New evidence for morphological and genetic variation in the cosmopolitan coccolithophore *Emiliania huxleyi* (Prymnesiophyceae) from the COX1b-ATP4 genes. *J. Phycol.* (in the press).
- Gibbs, S. J., Bown, P. R., Sessa, J. A., Bralower, T. J. & Wilson, P. A. Nannoplankton extinction and origination across the Paleocene–Eocene Thermal Maximum. *Science* **314**, 1770–1773 (2006).
- Monnin, E. *et al.* Atmospheric  $\text{CO}_2$  concentrations over the last glacial termination. *Science* **291**, 112–114 (2001).
- Petit, J. R. *et al.* Climate and atmospheric history of the past 420,000 years from the Vostok ice core, Antarctica. *Nature* **399**, 429–436 (1999).

Supplementary Information is linked to the online version of the paper at [www.nature.com/nature](http://www.nature.com/nature).

**Acknowledgements** We thank the crew from Puerto Deseado, Atalante, Suroit and Marion-Dufresne, and D. Vaulot, L. Garczarek, M.-A. Sicre and H. Claustre for their help in collecting material for this work. The long-term OISO observational programme is supported by INSU (Institut National des Sciences de l'Univers), IPSL (Institut Pierre-Simon Laplace) and IPEV (Institut Paul-Emile Victor). We thank F. C. Bassinot for help in estimating palaeosalinities. The IMAGES programme is acknowledged for collection and curation of the cores. This work was funded by the 'Agence National de la Recherche' project PALEO-CTD (grant ANR-06-JCJC-0142), by the European Research Council under grant agreement 205150, by the European Funding Agencies from the ERA-net program Biodiversa, under the Biomars project, and by the European Community's Seventh Framework Program EPOCA (European Project on Ocean Acidification) under grant agreement 211384.

**Author Contributions** On the basis of an original idea from L.B., the concept of this paper was developed in discussion between all authors. L.B., N.B., P.C. and M.G. conducted coccolith measurements, D.R.-P., N.M. and C.G. conducted modern-ocean chemistry measurements, L.B. and T.d.G.-T. computed past ocean chemistry, E.M.B., I.P. and C.d.V. performed genetic analyses, B.R., R.E.M.R. and I.P. conceptualized the physiological interpretation, L.B., I.P., D.R.-P., C.d.V. and R.E.M.R. interpreted the relationships between calcification and environment.

**Author Information** Reprints and permissions information is available at [www.nature.com/reprints](http://www.nature.com/reprints). The GenBank accession numbers are JN098138–JN098158, JN098160 and JN098163–JN098174; their correspondence is given in the online Supplementary Information. The authors declare no competing financial interests. Readers are welcome to comment on the online version of this article at [www.nature.com/nature](http://www.nature.com/nature). Correspondence and requests for materials should be addressed to L.B. ([beaufort@ceregr.fr](mailto:beaufort@ceregr.fr)).